Marie Skłodowska-Curie (MSCA) – Innovative Training Networks (ITN)
H2020-MSCA-ITN European Training Networks

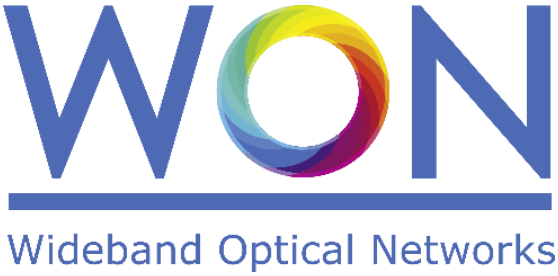

Wideband Optical Networks [WON]

Grant agreement ID: 814276

WP2 – Digital signal processing and system modelling

Deliverable D2.3 Digital signal processing for wideband optical systems

This project has received funding from the European Union's Horizon 2020 research and innovation programme under the Marie Skłodowska-Curie grant agreement 814276.

Document Details

Work Package	WP2 – Digital signal processing and system modelling
Deliverable number	D2.3
Deliverable Title	Digital signal processing for wideband optical systems
Lead Beneficiary:	POLITO
Deliverable due date:	31 December 2021
Actual delivery date:	10 February 2022
Dissemination level:	Public

Project Details

Project Acronym	WON
Project Title	Wideband Optical Networks
Call Identifier	H2020-MSCA-2018 Innovative Training Networks
Coordinated by	Aston University, UK
Start of the Project	1 January 2019
Project Duration	48 months
WON website:	https://won.astonphotonics.uk/
CORDIS Link	https://cordis.europa.eu/project/rcn/218205/en

WON Consortium and Acronyms

Consortium member	**Legal Entity Short Name**
Aston University	Aston
Danmarks Tekniske Universitet	DTU
VPIphotonics GmbH	VPI
Infinera Portugal	INF PT
Fraunhofer HHI	HHI
Politecnico di Torino	POLITO
Technische Universiteit Eidhoven	TUE
Universiteit Gent	UG
Keysight Technologies	Keysight
Finisar Germany GmnH	Finisar
Orange SA	Orange
Technische Universitaet Berlin	TUB
Instituto Superior Tecnico, University of Lisboa	IST

Abbreviations

PS:	Probabilistic shaping
CA:	Consortium Agreement
GA:	Grant Agreement
QAM:	Quadrature Amplitude Modulation
DSP:	Digital Signal Processing
CPE:	Carrier Phase Estimation
BPS:	Blind Phase Search
V&V:	Viterbi and Viterbi
ML:	Maximum Likelihood
CPR:	Carrier Phase Recovery
LUT:	Look-Up Table
MAP:	Maximum A Posteriori
AWGN:	Additive White Gaussian Noise
NGMI:	Normalized Generalized Mutual Information
RDE:	Radius Directed Equalizer
LBS:	Likelihood-Based Selection
CMA:	Constant Modulus Algorithm
STD:	Standard
PDF:	Probability Density Function
PMD:	Polarization Mode Dispersion
SOP:	State Of Polarization
POH:	Pilot Overhead
CME:	Constant Modulus Equalizer
QPSK:	Quadrature Phase Shift Keying
DGD:	Differential Group Delay
FDA:	Fully Data-Aided
NLIN:	Nonlinear Interference Noise
ResN:	Residual Noise
SSMF:	Standard Single Mode Fiber
NZDSF:	Non-Zero Dispersion Shifted Fiber
CS:	Cycle Slips
SS:	Single Stage
FW:	Fixed Window
VW:	Variable Window
DS:	Dual Stage

CONTENT

LIST OF FIGURES

EXECUTIVE SUMMARY

The present scientific deliverable is part of Work Package 2 “Digital signal processing and system modelling”, in turn part of the ETN project WON “Wideband Optical Networks”, funded under the Horizon 2020 Marie Skłodowska-Curie scheme Grant Agreement 814276.

This document provides details on the state-of-art digital signal processing improvements applied to probabilistic shaping constellation signals, which represent a promising solution in a multi-band scenario to finely and adaptively tune the information rate according to the local channel performance at each wavelength, thus maximizing the overall channel capacity. The main topics carried out and presented in this text are: (i) Two-stage blind phase recovery scheme tailored for probabilistically shaped QAM. (ii) A novel pilot-aided equalization technique based on the standard radius directed equalizer (iii) Quantification of achievable phase noise mitigation for different carrier phase recovery implementations.

1. Low complexity blind carrier phase recovery for probabilistically shaped QAM

In recent years, probabilistic shaping (PS) gained attention as a solution capable of delivery superior performance for coherent optical transmissions. This solution also brings some challenges, as it presents additional penalties from the digital signal processing (DSP) chain to the theoretical gain of quadrature amplitude modulation (QAM) [1]. The possible solutions are: (i) to use modulation-independent heavily pilot-based DSP or (ii) to apply standard blind algorithms developed for unshaped M-QAM. Because of that, blind carrier phase estimation (CPE) it is well accepted that the state-of-the-art for high order modulations is represented by the blind phase search (BPS) algorithm [2]. However, still considerably lower complexity solutions based on the simple Viterbi and Viterbi 4th power (V&V) and maximum likelihood phase estimators (ML) have been successfully implemented for unshaped modulation up to 16-QAM [3]. In [4] is proposed a two-stage carrier phase recovery (CPR) based on a modification of V&V and ML in which is used the knowledge about the a-priori transmitted symbol probabilities to perform an optimum symbol and amplitude level assignments.

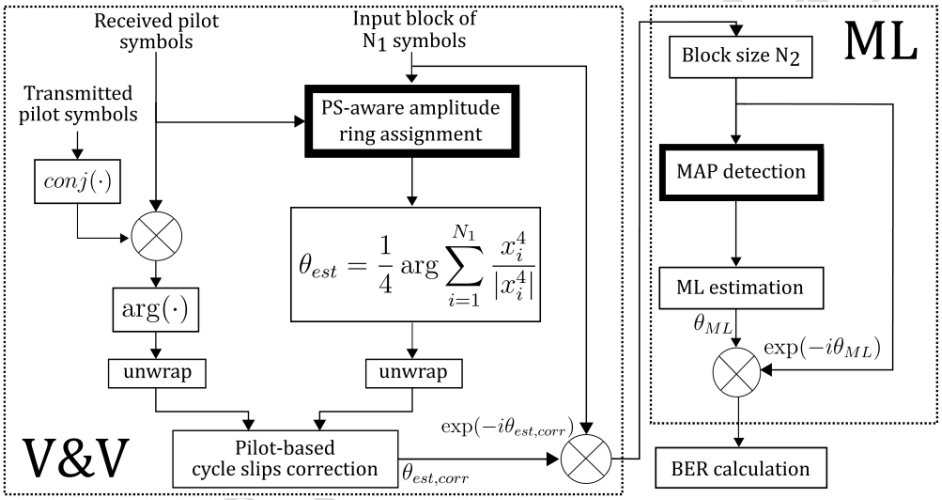

Figure 1: Block diagram of a two-stage CPR [4] based on V&V + ML.

In
Figure 1 is presented the proposed algorithm block diagram, in which the thicker black frames are the ones that differ with respect to the standard non PS-aware V&V + ML. The first block consists of a V&V 4th power CPE. For modulation formats higher than 4-QAM, amplitude discrimination over the received symbols must be performed. The optimum discrimination can be obtained by maximizing the probability that the received symbol with amplitude *A* belongs to the *k*-th constellation ring R_k among the possible *K* amplitude levels. For a given constellation entropy and estimated SNR, the maximization can be performed a-priori by defining the thresholds among different rings R_k, R_{k+1} *(k= 1 ... K−1)* as proposed in [5]. These values can be stored for the desired SNR range and granularity in a look-up table (LUT) for an efficient real-time implementation. The second block consists in a refining of the phase estimation through an additional ML stage. For PS-QAM an optimum maximum a posteriori probability (MAP) detection is used [6]. This approach is used for this ML stage and proves effective in reducing the number of symbol classification errors, in particular for low SNR [4].

Figure 2 is shown the simulated transmission of 2^{16} symbols modulated as 16-QAM-PS or 64-QAM-PS with variable entropy, ranging from 2.66 to 4.5.

Figure 2 (a-d) depict the penalty with respect to the SNR needed for obtaining a BER of 2.7×10^{-2} for the specified modulation format in the presence of additive white Gaussian noise (AWGN) only. We can notice that for both entropy scenarios with 16-QAM, the proposed algorithm outperforms both non PS-aware and BPS algorithms. For a higher modulation format (64-QAM) for entropy 4 case, the PS-aware algorithm outperforms both others till linewidth symbol-duration product of 10^{-4}. On the contrary, when the entropy is increased further, BPS shows an increased performance gain, confirming to be the best algorithm for higher order modulation formats [4].

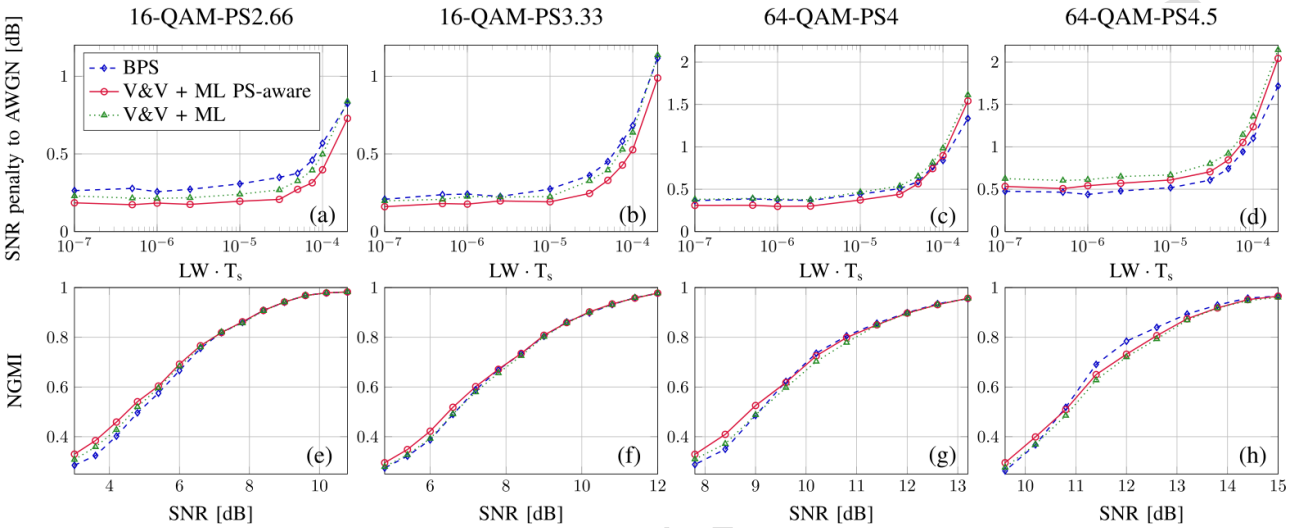

Figure 2: (a-d): SNR penalty of the implemented algorithms with respect to AWGN for BER = 2.7 × 10−2 versus the combined linewidth symbol-duration product. The AWGN SNR values considered are: $SNR_{0,2.66}$ = 7.35 dB, $SNR_{0,3.33}$ = 9.33 dB, $SNR_{0,4}$ = 10.60 dB, $SNR_{0,4.5}$ = 12.05 dB. (e-h): NGMI versus SNR for LW · T_s = 10−5, equivalent to a combined linewidth of 320kHz considering 32 Gbaud signals.

Figure 2 (e-h) shows the normalized generalized mutual information (NGMI) versus SNR for a linewidth symbol-duration product of 10^{-5}. Our algorithm is only outperformed by BPS in the 4.5 entropy case for high SNR values. At the same time, it shows a clear performance improvement with respect to standard V&V and BPS for low SNR values in all four entropy cases. Regarding the cost for implementation, BPS presents a higher complexity, which can be estimated as *B* times the one of a V&V stage [4]. The CPR parameters used in
Figure 2 (a-d) and shown in Table 1, in which *N* is the filter's block length.

Table 1: Parameters of the different CPR implementations

PARAMETERS OF THE DIFFERENT CPR IMPLEMENTATIONS

Constellation entropy	**2.66**	**3.33**	**4**	**4.5**
N V&V	150	130	130	120
N ML	50	50	50	50
N BPS	90	90	70	70
B	16	16	64	64

2. Likelihood-Based Selection Radius Directed Equalizer with Time-Multiplexed Pilot Symbols for Probabilistically Shaped QAM

As already mentioned in Section 1, PS QAM is a promising solution for coherent optical transmissions. For this scenario, channel equalization is a challenging operation, with pioneering works relying on fully data-aided solutions [7] and periodically transmitted training sequences [8]. In [9] is presented a novel pilot-aided algorithm for channel equalization based on the ubiquitous radius directed equalizer (RDE) using likelihood-based selection (LBS), in which the filter taps are updated upon reception of a sample only if the likelihood of its amplitude to be correctly assigned to a constellation level is sufficiently high.

Constant modulus algorithm (CMA) and standard-RDE (STD-RDE) are standard solutions for time-domain polarization demultiplexing and dynamic channel equalization when employing quadrature phase shift keying (QPSK) and multilevel QAM signals, respectively. For a MQAM constellation with K possible amplitude rings, these error functions can be calculated as [10]:

$$\epsilon_x[n] = R_k^2[n] - |x_{out}[n]|^2$$
$$\epsilon_y[n] = R_k^2[n] - |y_{out}[n]|^2$$

where $x_{out}[n]$ and $y_{out}[n]$ are the output of the equalizer in the two orthogonal polarizations. For STD-RDE, $R_k[n]$ is the constellation radius that is closest to the received *n*-th sample and depends on the transmitted MQAM constellation points A_m and the possible amplitude levels that they can assume R_k. For CMA however, $R_k[n]$ takes a single constant value equal to $R_0 = \sqrt{E[|A_m|^4/|A_m|^2]}$. Even with CMA being possible to be applied for multilevel constellations, STD-RDE has the advantage of optical error criteria [9], obtained throughout the Euclidian distance between the received sample amplitude *A* and the transmitted levels R_k. In presence of AWGN with variance σ^2 it is in fact possible to calculate the likelihood of a received symbol with amplitude *A* to belong to the ring R_k as a Rician distribution:

$$f(A|R_k) = \frac{A}{\sigma^2}\exp\left[\frac{-(A^2 + R_k^2)}{2\sigma^2}\right] I_0\left(\frac{AR_k}{\sigma^2}\right)$$

where $I_0(\cdot)$ is the 0[th] order of the Bessel function. Following the Bayes theorem, is possible to obtain the optimum discrimination, knowing the constellation rings probability density function (PDF) $f(R_k)$, by maximizing the probability that the received symbol with amplitude *A* belongs to the *k*-th constellation ring R_k among all possible *K* amplitude levels:

$$\max_{k\in 1,\dots,K}\big(f(R_k|A)\big) \Leftrightarrow \max_k\big(f(R_k)f(A|R_k)\big)$$

On the contrary of the STD-RDE, the LBS-RDE consider the relative likelihood, denotated α, of any received amplitude level to be correctly assigned to the determined radius:

$$\alpha(A) = \max_{k\in 1,\dots,K}\frac{f(R_k)f(A|R_k)}{\sum_{k=1}^{K} f(R_k)f(A|R_k)}$$

with $\alpha(A)$ providing information about how much the received sample can be trusted to lead to a correct update. In [9] a threshold α_{th} is defined to perform the filters updates only when the received samples amplitude $\alpha(A[n]) > \alpha_{th}$, showing that this threshold needs to be careful optimized, as a reduced update rate can discard sufficiently good samples and a high update rate can increase the assignment error rate.

All the approaches described so far are applied in fully blind STD-RDE algorithms. However, they can fail in scenarios characterized by large polarization mode dispersion (PMD), noise and/or dynamic state of polarization (SOP) rotations. Due to that, several pilot-aided solutions have been proposed, rely on transmitting periodically a short known data sequence with good spectral properties [11]. The results shown in this section made use of a pilot-aided CMA. In order to try to eliminate the weakness of the pilot-aided CMA, like penalty for low pilot overhead (POH) and seldom filters update which reduce the equalizer tracking speed over dynamic channels characterized by rapid SOP rotations, the blind update is performed by the LBS update rule for RDE and compared with the STD-RED and the constant modules equalizer (CME) using CMA.

The system in which the comparison is made is composed by MQAM-PS signals generated by probabilistic amplitude shaping (PAS) with length of 2^{17} symbols randomly drawn from a Maxwell-Boltzmann distribution described as:

$$f(A_i) = \frac{\exp\left(-\lambda {A_i}^2\right)}{\sum_{A_i \epsilon A_{I,Q}} \exp\left(-\lambda {A_i}^2\right)}$$

where $A_{I,Q}$ is the set of amplitude values that the *I* and *Q* components of the constellation and λ is a factor optimized in order to achieve the desired signal entropy $H = -\sum_{A_i \epsilon A_{I,Q}} f(A_i) \log_2[f(A_i)]$. The signals generated are based on 16QAM, 64QAM, and 256QAM with *H* = 3 bit/symbol (16QAM-PS3), 4 bit/symbol (64QAM-PS4) and 6 bit/symbol (256QAM-PS6). The MQAM-PS signals are assessed by the NGMI [12]. The signals have symbol rate of 32 Gbaud and are first periodically interleaved with QPSK pilots every *N* symbols. The pilot rate is set to either 1/32 or 1/128 in order to simulate conditions characterized by a relatively high and low POH. After the transmitter the noise is loaded, as shown in Figure 3, and pass by 30 spans of 100 km of standard single mode fiber with $D = 16$ ps / (nm km). Two deterministic birefringence profiles are set to provide differential group delay (DGD) of 12 and 60 ps, in order to simulate conditions characterized by moderate and large DGD. Finally, is introduced one lumped linear SOP rotation after 15 spans to emulate the impact of events such as lightning strikes in the vicinity of the fiber on the signal SOP. The receiver side is composed by coherent receiver and a chromatic dispersion compensation. After, the signal is equalized by one of the approaches described before, passes by a fully data-aided maximum-likelihood CPR, the pilot symbols are removed from the stream, and the NGMI is calculated over the received samples.

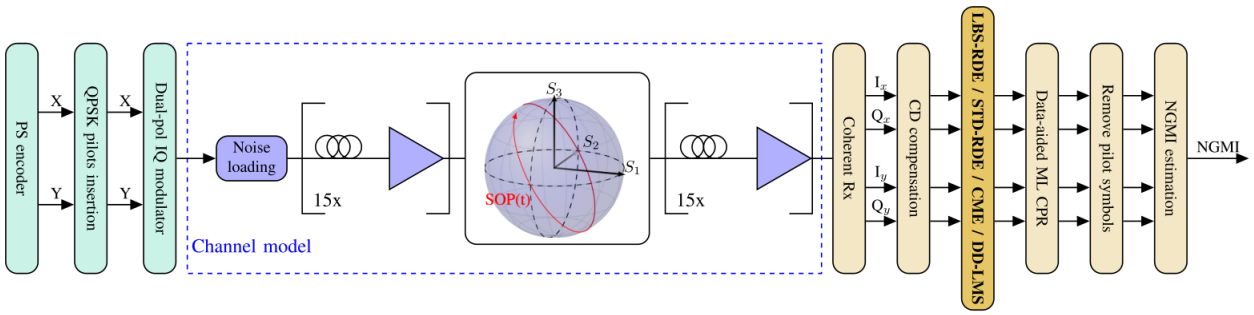

Figure 3: Illustration of the transmission system to evaluate the equalizers.

The first comparison, shown in Figure 4 and using VPIphotonics Design Suite 11 [13], is done for transmission over static channel with AWGN and fiber birefringence only with DGD=60 ps, two POH and three modulation formats, sweeping the SNR to obtain the NGMI between 0.7 and 1. All three equalizers discussed above, CME, STD-RDE and LBS-RDE, are compared with the fully data-aided implementation of the conventional RDE (FDA-RDE), which is the limiting best case scenario. For 16QAM-PS3 case in Figure 4(a,b), is noticeable that for higher POH, all the equalizers perform equally well, close to the FDA-RDE limit. However, for lower POH we notice that STD-RDE stars to fail for SNR < 7 dB. Moreover, CME presents a penalty, compared with LBS-RDE and FDA-RDE, for almost all analysed range. Going for 64QAM-PS4 in Figure 4(c,d), higher POH presents the same behaviour as the previous case. For lower POH, two characteristics can be noticed: firstly, the STD-RDE is not plotted as it does not provide a reliable convergence over most of the range, making it unsuitable for this application and secondly, the proposed LBS-RDE presents a penalty like CME for lower SNR values and almost no penalty for higher SNR values. Again, CME presents a penalty for all range analysed. Finally in Figure 4(e,f) the results for 256QAM-PS6 are shown, in which for higher POH the equalizer behaves similar. For lower POH, again the STD-RDE is unsuitable for these signals and for SNR < 15 and, CME and LBS-TDE presents the same performance. For higher SNR values, the LBS-RDE outperform CME for NGMI > 0.9.

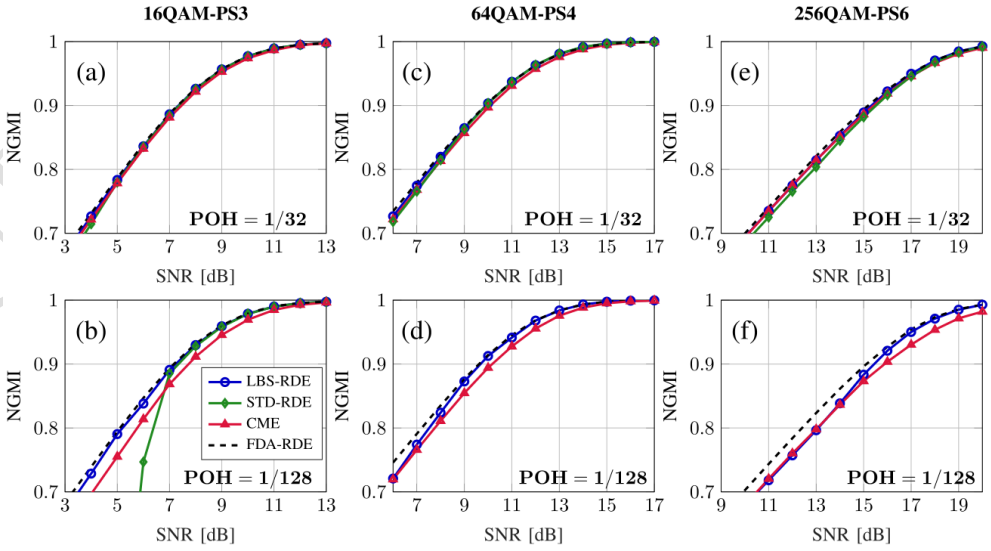

Figure 4: Performance in static conditions: NGMI versus SNR for the equalizers under test for the different shaped modulation format tested and POH of 1/32 and 1/128.

In Figure 5 are presented the SNR penalty needed to preserve the NGMI > 0.88 compared to the ideal FDA-RDE results in static conditions versus the SOP rotation rate applied in a transmission which the signal is submitted to a rapid linear rotation. Two DGD values are used. In Figure 5(a) we notice that both solutions with payload for the filters update outperforms the CME, with lower SNR penalties presented by LBS-RDE for both DGD values tested. Going for Figure 5(b), is possible to see a huge impact on CME and STD-RDE, allowing a maximum SOP rotation rate of around 0.5 and 1.5, respectively. The LBS-RDE algorithm presented a penalty increase if compared with higher POH, but still smaller than the others. In Figure 5(c, d) are shown the results for 64QAM-PS4. For higher POH case, both CME and STD-RDE have a similar performance, mainly due to the increasing in constellation energy which improves the CME [9]. For lower POH, similarly to the results presented in Figure 4, the STD-RDE is not plotted and LBS-RDE being able to endure SOP rotation rates up to 1.5 for DGD = 60 ps.

Finally, in Figure 5 (e, f) the results for 256QAM-PS6 are shown. For higher POH, the LBS-RDE outperform all other cases, with CME performing better than STD-RDE. In case of lower POH, the same performance is observed. These results shown that the LBS-RDE is the best algorithm for both static and dynamic SOP conditions.

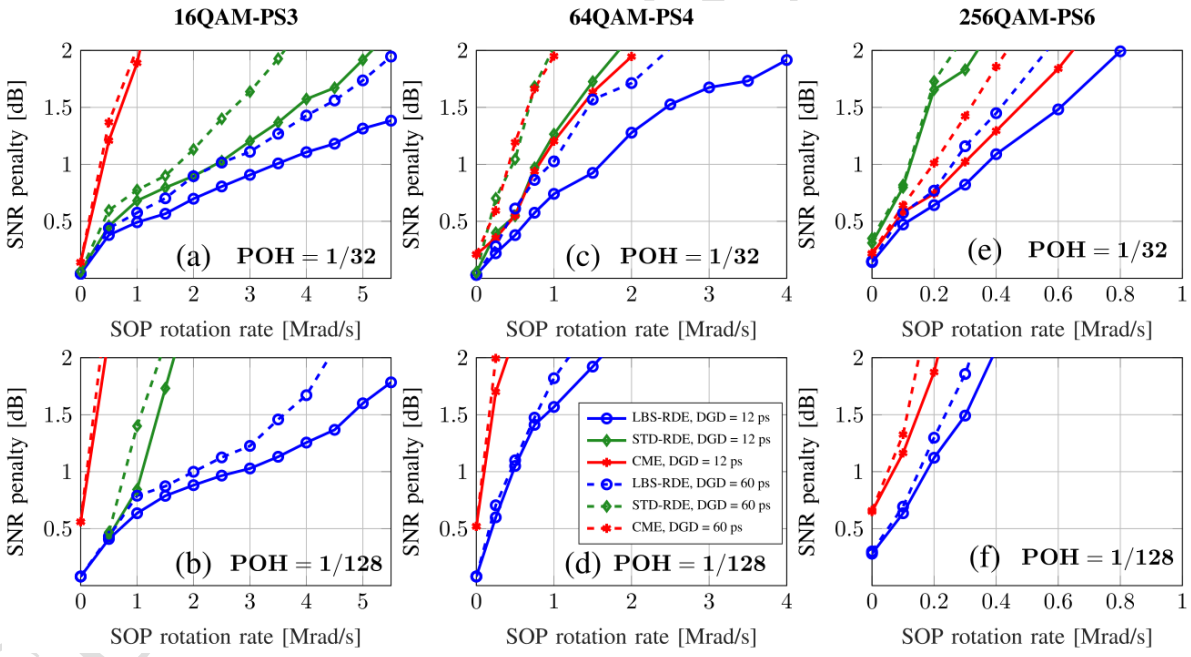

Figure 5: Performance in dynamic SOP conditions: SNR penalty with respect to ideal fully data-aided equalization over a static channel to preserve NGMI > 0.88. The reference SNR values for the different cases are: (a) 6.84 dB, (b) 6.71 dB, (c) 9.35 dB, (d) 9.10 dB, (e) 14.61 dB, (f) 14.52 dB.

3. Achievable Mitigation of Nonlinear Phase Noise through Optimized Blind Carrier Phase Recovery

One key aspect of optical transmission is the impairment caused by the Kerr nonlinearity, which can be a limiting factor of the optical transmission capacity [14] and is referred as nonlinear interference noise (NLIN). This effect can be divided into two components, the nonlinear phase noise component (NLPN) and the residual noise (ResN). The former can be almost entirely cancelled by the CPR while only the ResN remains on the constellation after the DSP. In order to evaluate the NLPN mitigation by the CPR, a comparison is performed in [15] considering the interplay of the nonlinear and linear impairments in defining the optimized parameters of the phase estimation algorithm.

The analysis is done using the VPIphotonics Design Suite 10.1 [13]. Five signals are simulated around the central frequency of 1550 nm with space of 50 GHz and symbol rate of 32 Gbaud. The modulation format used is PS 64-QAM with target entropy of 4.5. The selected modulation format aims the observation of conditions in which the NLPN is expected to have a significant contribution to the overall system performance. The signals are launched with 0 dBm of input power through 20 spans of 80 km each. Two fiber types are analysed: (a) standard single mode fiber (SSMF) with attenuation of 0.2 dB/km, dispersion of 16 ps / (nm km), nonlinear coefficient of 1.3 W^{-1} km^{-1} and effective area of 80 µm2, and (b) non-zero dispersion shifted fiber (NZDSF) with same attenuation, dispersion of 3 ps / (nm km) and same nonlinear coefficient and effective area. After each span the amplifiers recover the input power, presenting a noise figure of 5 dB.

Using a feedforward BPS algorithm on the CPR, two parameters can be tunned: N_p representing the number of test phases to rotate the received constellation, and N_w representing the window size in order to estimate block-wise the test phase for which the distance among the rotated points and their decisions over the ideal constellation points is minimized. To keep the cycle slips (CS), which can have a destructive impact on the received symbols [16], probability sufficient low, three CPR implementations are compared: (1) a single stage BPS with fixed window length (SS-FW) of N_w=50, (2) a single stage BPS with variable window length (SS-VW), optimizing N_w to minimize the symbol error rate (SER), and (3) dual stage BPS (DS) with N_w=50 for the first stage and optimization to follow the dynamics of the phase noise by minimizing the SNR [17] for the second stage. The ideal phase noise cancelation is also shown to be use as reference case [18]. As the parameter N_p is close related to more accurate phase noise mitigation but also to an increasing in hardware complexity and power consumption, N_p=16 and N_p=64 parameters are tested.

In
Figure 6 is presented the all the SSFM results, showing the SNR and SNR penalty, both versus number of fiber spans. Firstly, we can see that the BPS DS outperform all the other two single stage BPS. For long distances (distance > 15 spans), we can see that the solutions perform close to each other, with almost no penalty improvement with the number of test phases increasing. Regarding medium transmission distance (5 < distance < 15), we can already see the bad performance of the SS-FW as well as the performance of DS achieving the theoretical phase noise mitigation, with less than 0.1 dB of SNR penalty for N_p=64. For short distances this penalty is higher, again with the worst performance provided by the SS-FW. The number of test phases increasing provide an improvement in all cases, with the DS performing better than the others. In
Figure 7 the analysis for transmission using NZDSF is shown, with almost the same conclusions of the SSFM results. It is clear however, these results present higher penalties, especially for medium

and long-haul transmissions. The lower dispersion in the fiber in fact reduces the interaction among pulses for a given transmission distance and at the same time enhances NLIN. The results shown that a two stage CPR outperforms single stage solutions by combining resilience to cycle slips while at the same time following better the dynamics of short-correlated NLPN [15].

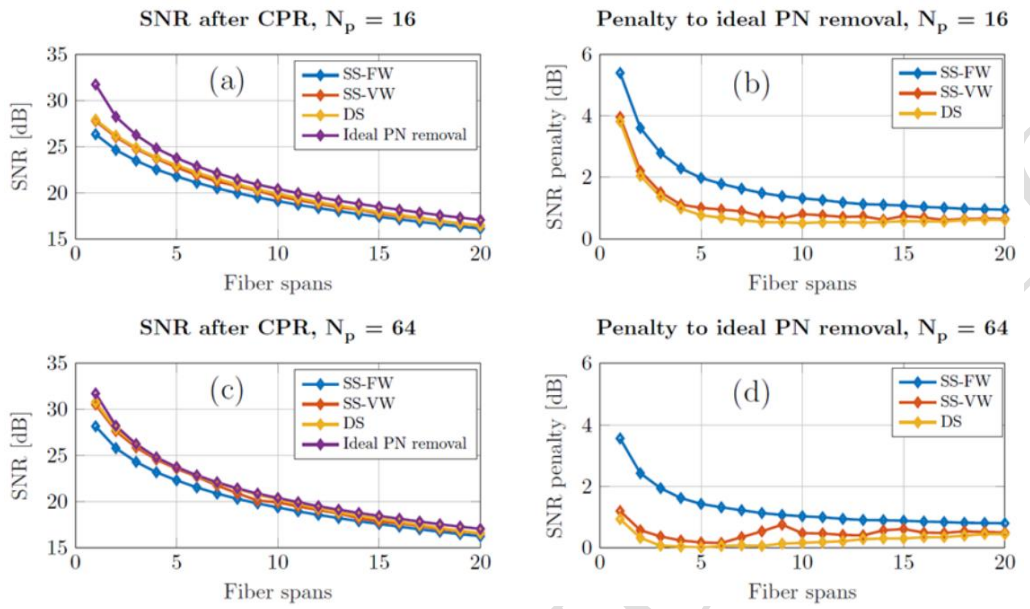

Figure 6: (a,c) SNR after the proposed CPR implementations and ideal phase noise removal; (b,d) SNR penalty of the CPR implementations with respect to ideal phase noise removal. All data for transmission over SSMF.

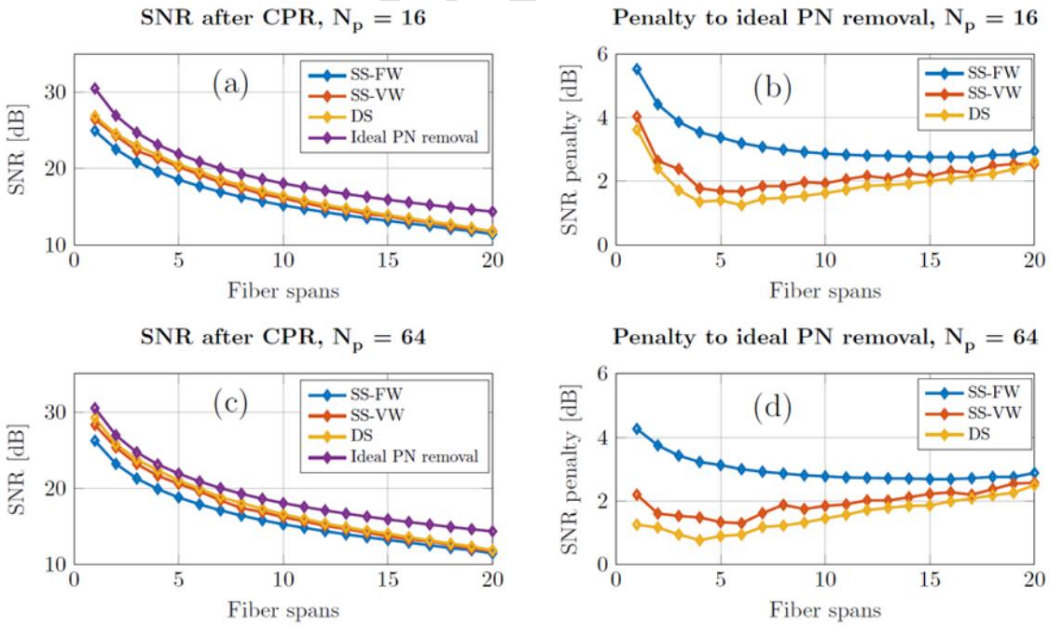

Figure 7: (a,c) SNR after the proposed CPR implementations and ideal phase noise removal; (b,d) SNR penalty of the CPR implementations with respect to ideal phase noise removal. All data for transmission over NZDSF.

4. Conclusions

In this work, we presented digital signal processing improvements applied to probabilistic shaping constellation signals, which represent a promising solution for capacity-achieving multi-band coherent optical transmission systems. The solutions presented in section 1 and 2. Allow to adapt the DSP operation to perform better by considering local channel performance, taking into consideration spectral bands characteristics. In section 3, we presented a study of the achievable performance of state-of-the-art carrier phase recovery compared to a validated statistical method able to provide phase-agnostic system performance [18]. The analysis is performed for different amounts of chromatic dispersion, which represents a crucial variable in the context of ultra-wideband transmission systems.

It is important to highlight that the results and approaches presented in this deliverable are summaries that contain only a subset of obtained results. Additional details can be found in other recent publications by the project contributors [4] [9] [15].

5. REFERENCES

[1] F. A. Barbosa, S. M. Rossi und D. A. A. Mello, "Phase and frequency recovery algorithms for probabilistically shaped transmission", *Journal of Lightwave Technology,* Bd. 38, Nr. 7, p. 1827–1835, 1 Apr 2020.

[2] T. Pfau, S. Hoffmann und R. Noe, "Hardware-Efficient Coherent Digital Receiver Concept With Feedforward Carrier Recovery for M-QAM Constellations", *Journal of Lightwave Technology,* Bd. 27, Nr. 8, pp. 989-999, 2009.

[3] K. Zhong, J. H. Ke, Y. Gao und J. C. Cartledge, "Linewidth-Tolerant and Low-Complexity Two-Stage Carrier Phase Estimation Based on Modified QPSK Partitioning for Dual-Polarization 16-QAM Systems", J. Lightwave Technol., Bd. 31, Nr. 1, pp. 50--57, Jan 2013.

[4] G. Di Rosa und A. Richter, "Low Complexity Blind Carrier Phase Recovery for Probabilistically Shaped QAM", IEEE Photonics Technology Letters, Bd. 32, Nr. 17, pp. 1109-1112, 2020.

[5] S. Dris, S. Alreesh und A. Richter, "Blind Polarization Demultiplexing and Equalization of Probabilistically Shaped QAM", in 2019 Optical Fiber Communications Conference and Exhibition (OFC), 2019.

[6] S. Hu, W. Zhang, X. Yi, Z. Li, F. Li, X. Huang, M. Zhu, Jingzhang und K. Qiu, "MAP Detection of Probabilistically Shaped Constellations in Optical Fiber Transmissions", in 2019 Optical Fiber Communications Conference and Exhibition (OFC), 2019.

[7] F. Buchali, F. Steiner, G. Böcherer, L. Schmalen, P. Schulte und W. Idler, "Rate Adaptation and Reach Increase by Probabilistically Shaped 64-QAM: An Experimental Demonstration", Journal of Lightwave Technology, Bd. 34, Nr. 7, pp. 1599-1609, 2016.

[8] Y. Zhu, A. Li, W.-R. Peng, C. Kan, Z. Li, S. Chowdhury, Y. Cui und Y. Bai, "Spectrally-efficient single-carrier 400G transmission enabled by probabilistic shaping", in 2017 Optical Fiber Communications Conference and Exhibition (OFC), 2017.

[9] G. Di Rosa und A. Richter, "Likelihood-Based Selection Radius Directed Equalizer With Time-Multiplexed Pilot Symbols for Probabilistically Shaped QAM", Journal of Lightwave Technology, Bd. 39, Nr. 19, pp. 6107-6119, 2021.

[10] M. S. Faruk und S. J. Savory, "Digital Signal Processing for Coherent Transceivers Employing Multilevel Formats", Journal of Lightwave Technology, Bd. 35, Nr. 5, pp. 1125-1141, 2017.

[11] M. Nölle, F. Frey, R. Elschner, C. Schmidt-Langhorst, J. K. Fischer und C. Schubert, "Investigation of CAZAC sequences for data-aided channel estimation considering nonlinear optical transmission", in 2015 Optical Fiber Communications Conference and Exhibition (OFC), 2015.

[12] J. Cho, L. Schmalen und P. J. Winzer, "Normalized Generalized Mutual Information as a Forward Error Correction Threshold for Probabilistically Shaped QAM", in 2017 European Conference on Optical Communication (ECOC), 2017.

[13] "https://vpiphotonics.com/Tools/DesignSuite/", [Online].

[14] R.-J. Essiambre, G. Kramer, P. J. Winzer, G. J. Foschini und B. Goebel, "Capacity Limits of Optical Fiber Networks", Journal of Lightwave Technology, Bd. 28, Nr. 4, pp. 662-701, 2010.

[15] G. di Rosa und A. Richter, "Achievable Mitigation of Nonlinear Phase Noise through Optimized Blind Carrier Phase Recovery", in 2020 22nd International Conference on Transparent Optical Networks (ICTON), 2020.

[16] E. Börjeson und P. Larsson-Edefors, "Cycle-Slip Rate Analysis of Blind Phase Search DSP Circuit Implementations", in 2020 Optical Fiber Communications Conference and Exhibition (OFC), 2020.

[17] A. Bisplinghoff, C. Vogel, T. Kupfer, S. Langenbach und B. Schmauss, "Slip-reduced carrier phase estimation for coherent transmission in the presence of non-linear phase noise", in 2013 Optical Fiber Communication Conference and Exposition and the National Fiber Optic Engineers Conference (OFC/NFOEC), 2013.

[18] G. D. Rosa, S. Dris und A. Richter, "Statistical quantification of nonlinear interference noise components in coherent systems", Opt. Express, Bd. 28, Nr. 4, pp. 5436--5447, 2020.